Development 134, 3099-3109 (2007) doi:10.1242/dev.004788

Haploinsufficiency after successive loss of signaling reveals a role for *ERECTA*-family genes in *Arabidopsis* ovule development

Lynn Jo Pillitteri, Shannon M. Bemis, Elena D. Shpak* and Keiko U. Torii†

The *Arabidopsis* genome contains three *ERECTA*-family genes, *ERECTA* (*ER*), *ERECTA-LIKE 1* (*ERL1*) and *ERL2* that encode leucine-rich repeat receptor-like kinases. This gene family acts synergistically to coordinate cell proliferation and growth during above-ground organogenesis with the major player, *ER*, masking the loss-of-function phenotypes of the other two members. To uncover the specific developmental consequence and minimum threshold requirement for signaling, *ER*-family gene function was successively eliminated. We report here that *ERL2* is haploinsufficient for maintaining female fertility in the absence of *ER* and *ERL1*. Ovules of the haploinsufficient *er-105 erl1-2 erl2-1/+* mutant exhibit abnormal development with reduced cell proliferation in the integuments and gametophyte abortion. Our analysis indicates that progression of integument growth requires ER-family signaling in a dosage-dependent manner and that transcriptional compensation among ER-family members occurs to maintain the required signaling threshold. The specific misregulation of cyclin A genes in the *er-105 erl1-2 erl2-1/+* mutant suggests that downstream targets of the ER-signaling pathway might include these core cell-cycle regulators. Finally, genetic interaction of the *ER* family and the WOX-family gene, *PFS2*, reveals their contribution to integument development through interrelated mechanisms.

KEY WORDS: *Arabidopsis*, Integument growth, Ovule, Receptor-like kinase, Haploinsufficient, Cell proliferation

INTRODUCTION

The final size and shape of plant organs are determined by developmental programs that coordinate cell proliferation, cell expansion and cell-type differentiation (Mizukami, 2001; Potter and Xu, 2001). The *Arabidopsis* ovule has a relatively simple structure and a specific, well-defined differentiation pattern, making it a useful model for understanding the regulation of growth and organogenesis. The ovule originates from the placenta as an elongate protrusion with a defined proximal/distal axis that can be separated into three regions. The distal portion, called the nucellus, is the site of megasporogenesis and embryo sac development. The proximal region differentiates into the funiculus or stalk, which attaches the ovule to the carpel wall. Two integuments initiate at the central chalazal region and eventually envelop the nucellus and form the seed coat. Similar to the process of leaf laminar expansion, initiation and expansion of the integument requires the juxtaposition of abaxial and adaxial factors such as those encoded by *PHABULOSA* (*PHB*), *KANADI1* (*KAN1*), *KAN2* and *KAN3*, *ABERRANT TESTA SHAPE* (also known as *KAN4* – TAIR), and the YABBY-family member *INNER NO OUTER* (Eshed et al., 2001; Eshed et al., 2004; McAbee et al., 2006; Sieber et al., 2004; Villanueva et al., 1999). In addition, transcription factors such as AINTEGUMENTA and NOZZLE (also known as SPOROCYTELESS), and the mitochondria ribosomal protein HUELLENLOS, have been identified as necessary for integument initiation (Elliott et al., 1996; Schneitz et al., 1998; Skinner et al., 2004; Villanueva et al., 1999).

A second group of loci affect the progression of integument growth after initiation. Several genes, including *PRETTY FEW SEEDS 2* (*PFS2*), *SHORT INTEGUMENTS 1* and *2* (*SIN1* and *2*) and *TSO1*, affect cell proliferation or expansion of the integuments, and their loss-of-function mutations result in reduction or loss of fertility (Hauser et al., 2000; Park et al., 2004; Park et al., 2005; Schneitz et al., 1997). Embryo sac failure is a secondary consequence of the absence of integuments; the gametophyte fails to develop in cases where the nucellus is not enclosed (Gasser et al., 1998). The cause of gametophyte abortion is not clear, but is likely to lie in the requirement for tight coordination of cell division and expansion within the ovule and communication between gametophytic and sporophytic tissue (Gasser et al., 1998). Relatively little is known about the genes involved in the coordination of growth or cell-cell communication within the ovule. This might be due to redundancy among the genes involved in this process, or to pleiotropic effects resulting from the loss of these genes. For instance, *TSO1*, *TOUSLED* (*TSL*) and *SIN1* have multiple, sometimes detrimental, effects on vegetative and floral development in addition to ovule defects (Ehsan et al., 2004; Lang et al., 1994).

ERECTA (*ER*) and its two paralogs, *ERECTA-LIKE 1* (*ERL1*) and *ERL2*, regulate organ shape and inflorescence architecture and are members of the leucine-rich repeat receptor-like kinase (LRR-RLK) gene family in *Arabidopsis* (Shiu and Bleecker, 2001; Torii, 2004; Torii et al., 1996). Based on phylogeny, it was suggested that *ERL1* and *ERL2* evolved by recent gene duplication and are functionally related to *ER*, while maintaining overlapping but unique transcript expression patterns (Shpak et al., 2004). We report here that in the absence of functional *ER* and *ERL1*, *Arabidopsis* plants heterozygous at the *ERL2* locus exhibit specific defects in integument development. Based on data from genetic and gene expression analysis, the ER family plays a key role in ovule development and fertility by regulating cell proliferation in the integuments. Our study highlights the unequal redundancy and dosage compensation among *ER*-family genes, and further reveals

Department of Biology, University of Washington, Seattle WA 98195 USA.

*Present address: Department of Biochemistry and Cellular and Molecular Biology, University of Tennessee, Knoxville, TN 37996, USA
†Author for correspondence (e-mail: ktorii@u.washington.edu)

Accepted 20 June 2007

a potential molecular consequence of their reduced dosage for cell division control of integument development and fertility. Finally, genetic interactions of the *ER* family with *PFS2*, a *WUSCHEL* (*WUS*)-type homeodomain gene, revealed an unexpected intersection of two pathways required for proper integument growth and embryo sac development.

MATERIALS AND METHODS

Plant material and growth conditions

The *Arabidopsis thaliana* ecotype Columbia (Col) was used as wild type. All mutants are in the Col background unless otherwise indicated. The *er-105*, *erl1-2* and *erl2-1* mutations were described previously (Shpak et al., 2004). The *erl1-1* allele (YJ133) was identified as an enhancer-trapped line by Dr John Bowman (University of California, Davis, CA) and kindly provided as a gift. The line was originally in the Landsberg *erecta* (L*er*) background and outcrossed into Col three times. The *erl1-4* allele was isolated from ethyl methanesulfonate-mutagenized *Arabidopsis er-105 erl2* seeds and outcrossed to Col. The *pfs2-1* allele was a gift from Dr Bernard Hauser (University of Florida, Gainesville, FL) and was in the L*er* background and outcrossed to Col. The *pfs2-1* mutant was crossed with the *er-105 erl1-2* (+/–) *erl2-1* mutant for further analysis. All plants were grown under long-day conditions as described previously (Shpak et al., 2003).

Genotyping

PCR-based genotyping for *er-105*, *erl1-2* and *erl2-1* mutations was described previously (Shpak et al., 2004). Detection of the *erl1-1* T-DNA insertion was performed with PCR primers: ERLK-185.rc, 5′-CGTAGGTCTCCAATACGTGGA-3′ and GUS R, 5′-CAGTTGCA-ACCACCTGTTGAT-3′. The *erl1-4* mutation was detected by derived Cleaved Amplified Polymorphic sequences (dCAPs) using primers: erl1-4dcaps1151, 5′-GACGATGTTCACAACAGTGACTTGTGTTCTAG-3′ and erl1-4dcaps1447.rc, 5′-CATCGAAATCAACAGAGAAAGAAAGGG-3′, and subsequent digestion with *Xba*I for 2 hours at 37°C, which cuts the mutant *erl1-4* allele sequence.

In situ hybridization

Tissue preparation and in situ hybridization were performed as described previously (McAbee et al., 2006). Probe template construction was performed as follows. For the *ERL1* probe template, the *ERL1* sense and antisense probes were produced by linearizing plasmid pLJP562 (contains *ERL1* kinase domain) with *Bam*HI or *Xho*I and transcribing in vitro with T3 or T7 RNA polymerase, respectively. For the *ER* probe template, the *ER* sense and antisense probes were synthesized by linearizing pLJP131 (contains the *ER* kinase domain and partial 3′UTR) with *Xho*I or *Bam*HI and transcribing in vitro with T3 or T7 RNA polymerase, respectively. The *WUS* sense and antisense probes were produced by linearizing pSMB106 (nt 627-816 of the *WUS* cDNA) with *Eco*RI and *Xba*I and transcribing in vitro with T3 or T7 RNA polymerase, respectively. *PFS2* probe template construction and hybridization conditions were according to Park et al. (Park et al., 2005). Sense and antisense probes for *PHB* were produced by linearizing plasmid pPHB (a gift from Dr Kiyotaka Okada, Kyoto University, Kyoto, Japan) with *Sac*I or *Kpn*I and transcribing in vitro with T7 or T3 RNA polymerase, respectively.

GUS histochemical analysis

proERL1::GUS and *proERL2::GUS* constructs were described previously (Shpak et al., 2004). Histochemical staining for β-glucuronidase (GUS) activity was performed as described previously (Sessions et al., 1999).

RNA extraction and quantitative real-time RT-PCR

Total RNA was isolated from *Arabidopsis* stage 12 gynoecia (Schneitz et al., 1995) or from ovules isolated from stage 12 gynoecia using the RNeasy Plant Mini Kit (Qiagen, Valencia, CA) and treated with DNase I (Amp Grade, Invitrogen). First-strand cDNAs were generated by ThermoScript Reverse Transcriptase (Invitrogen) and random hexamers using 1.0 μg of RNA according to manufacturer's instructions. Real-time PCR was performed with a Chromo4 thermocycler (BioRad, Hercules, CA) and analyzed using Opticon Monitor 3 software (BioRad). Triplicate reactions were performed in 25 μl total volume containing iTaq SYBR Green mix (BioRad) and 1.0 μl of the first-strand reaction. *ACTIN 2* was used as an internal control in parallel reactions for each run. The relative level of expression of each target gene was calculated with respect to *ACTIN 2* expression for each genotype. Real-time reactions were repeated in two biological replicates and the average fold-difference relative to wild type was calculated. Oligomers and DNA sequences used for PCR are shown in Table 1.

Table 1. Primers for RT-PCR and probe synthesis

	Primer	Sequence (5′ to 3′)
Real-time RT-PCR primers		
ERECTA	sbr ER F	GACTGGACAACTTCACCTTCTTCG
	sbr ER R	GAACAGTCACCAATCTCATCAGG
ERL1	sbr ERL1 F	GAACTGCTTCACTCTTGTCAATCTG
	sbr ERL1 R	CATACCTGGCTGGAGCAAAACG
ERL2	ERL2 3085	CTGTCTGGCAACAATTTCTCA
	sbr ERL2 R	AACACGTACAGATTGGCAAGAC
ACTIN	sbr actin F	ATGTCGCCATCCAAGCTGTTCTC
	sbr actin r	CTCCTTGATGTCTCTTACAATTTCC
PFS2	pfs2 F	ATGGGCTACATCTCCAACAA
	sbr PFS2 R	CTTCTAGCGTCGTGATCTGC
CYCLIN A2;2	sbr CYCA22 F	GAGCTAAAAAAGCCATGGGAA
	sbr CYCA22 R	CACCTGATCCATCTTCTTGTTGC
CYCLIN A2;3	CYCA23 21	GTCTCGGCCATTCACTCG
	sbr CYCA23 R	TTTGGCCTCAAGTATACCTG
RT-PCR primers		
CYCLIN A2;1	CYCA21 153	GAAGCGTGTTGCTAGACCG
	CYCA21 347.rc	CTACCAAACCATCTTCTTC
CYCLIN A2;2	CYCA22 597	GCTAAAAAAGCCATGGGAAGA
	CYCA22 1103.rc	TGCTCAGTAATTTCTTCATCTT
CYCLIN A2;3	CYCA23 21	GTCTCGGCCATTCACTCG
	CYCA23 359.RC	CCTGCTGTATTTGATGCAAC
CYCLIN A2;4	CYCA24 (–26)	TTGGATCGTGTCAAAGGG
	CYCA24 518.rc	ACTTCTCTCAACTGTCCC
CDKB1;1	cdkb11 610	CAATGGCCGGGTGTTTCC
	cdkb11 +69.rc	TGTCGGAAAGAAAGATAG
CDKB1;2	cdkb12 615	CAATGGCCGGGTGTAATG
	cdkb12 +68.rc	GAGCAATAAACTTGACGG
CDKB2;1	cdkb21 (–40)	AGAGAGAGAGAGCGCCG
	cdkb21 352.rc	GAATGTTCTTGCCAGTGCT
CDKB2;2	cdkb22 (–32)	GAGAGAAGAGTTGTCTTG
	cdkb22 358.rc	GAATGTTCTGTCCAGCTTG
ERECTA	ER 2248	AAGAAGTCATTCAAAGATGTGA
	ER3016.rc	AGAATTTCCAGGTTTGGAATCTGT
ERL1	ERL1 2846	TATCCCACCGATACTTGGCA
	ERL1 4411.rc	CCGGAGAGATTGTTGAAGGA
ERL2	ERL2 3085	CTGTCTGGCAACAATTTCTCA
	ERL2 4254.rc	AGCCATGTCCATGTGAAGAA
ACTIN 2	act2-1	GCCATCCAAGCTGTTCTCTC
	act2-2	GCTCGTAGTCAACAGCAACAA
PFS2	pfs2 F	ATGGGCTACATCTCCAACAA
	pfs2 R	TCAGTTCTTCAGAGGCATGA
In situ hybridization probe primers		
ERECTA	ER 7040	GTAAAGATCTCGGTGTGG
	ER 7467.rc	GAAGACACATATTCACACC

Microscopy

Pictures of plants were taken with an Olympus SZX12 dissecting microscope attached to an Olympus C-2020Z digital camera (Center Valley, PA). Tissue fixation, plastic embedding, sectioning, light- and scanning electron microscopy were performed as described previously (Shpak et al., 2003). To examine ovules using differential interference contrast (DIC) optics, carpels were dissected from flowers and incubated in 9:1 (v:v) ethanol:acetic acid overnight, rinsed with water and placed in choral hydrate (1:8:1 v:v glycerol:chloral hydrate:water). Cleared ovules and in situ hybridization sections were viewed under DIC optics using an Olympus BX51 microscope equipped with a DP70 digital camera.

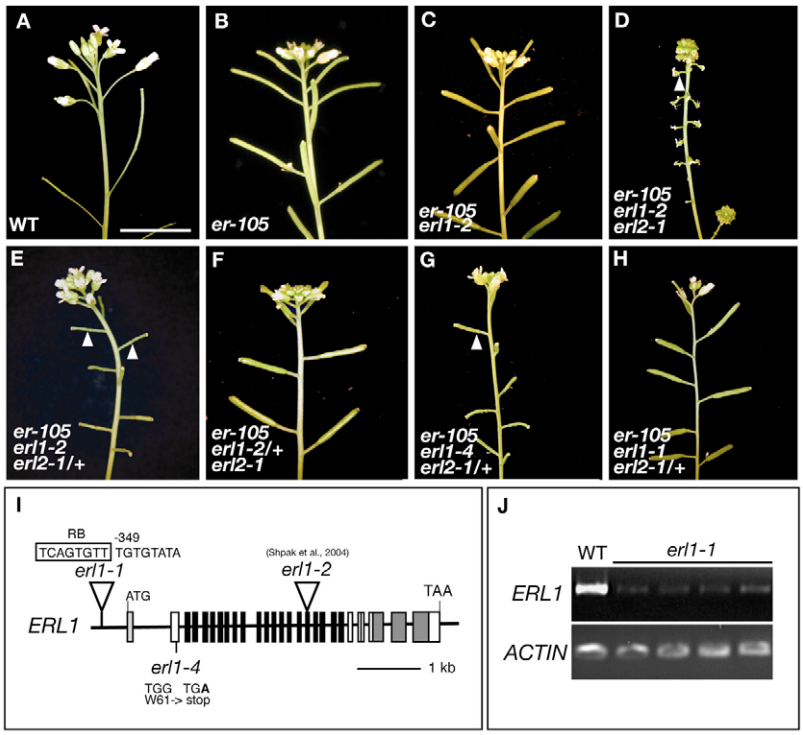

Fig. 1. Growth phenotype of wild-type and *er*-family mutant *Arabidopsis*. (**A-H**) Wild-type and *er*-family mutant inflorescence stems. (A) Wild type (WT); (B) *er-105*; (C) *er-105 erl1-2*; (D) *er-105 erl1-2 erl2-1*; (E) *er-105 erl1-2 erl2-1/+*; (F) *er-105 erl1-2/+ erl2-1*; (G) *er-105 erl1-4 erl2-1/+*; and (H) *er-105 erl1-1 erl2-1/+*. Wild type and all combination mutants (A-C,E-F) except *er-105 erl1-2 erl2-1* triple mutant (D) maintain proper floral organ patterning and elongation. Among the combinations, *er-105 erl1-2 erl2-1/+* (E), *er-105 erl1-4 erl2-1/+* (H) and the triple mutant (D), are female sterile. Scale bar: 1 cm. (**I**) Schematic of the *ERL1* gene with location of T-DNA insertions for *erl1-1* and *erl2-1*, and the point mutation for *erl1-4*. Exons are indicated as vertical bars, introns as lines. The T-DNA right border (RB) is boxed. (**J**) RT-PCR analysis of four separate *erl1-1* plants with reduced levels of *ERL1* transcript compared with wild type. *ACTIN 2* serves as a positive control.

Cell size and number measurements

Cell size was measured from images of plastic-embedded sections of wild-type and *er erl1-2 erl2-1/+* carpels. The length and width of the first ten cells (nucellar to chalazal end) of the outer layer of the outer integument were measured using pixel distance in Photoshop Pro (Adobe Systems, San Jose, CA). Images used for these measurements corresponded to similar cross-sections through the nucellus of mature wild-type and *er erl1-2 erl2-1/+* ovules. Cell numbers were counted from cleared ovules at stages 1-II, 2-IV, 3-II and 3-VI (Schneitz et al., 1995). At stages 2-IV, 3-II and 3-VI, counting started at the tip of the outer integument (nucellar end) and stopped where cells of the funiculus appeared obvious. At stage 1-II, all cells in the L1 layer of the ovule primordia were counted.

RESULTS

ERL2 is haploinsufficient for female fertility in the absence of *ER* and *ERL1*

As reported previously, *er*, *er erl1* and *er erl2* null mutants developed compact but otherwise normal inflorescences, whereas the loss of all *ER*-family genes led to extremely dwarf and sterile plants with aberrant flowers disrupted in organ patterning and differentiation (Shpak et al., 2004) (Fig. 1A-D). To unravel the specific functions of *ERL1* and *ERL2* during inflorescence and floral organ growth, we investigated the phenotypes conferred by reduced dosages of *ERL1* and *ERL2* in the absence of *ER*. For this purpose, 100 self-fertilized progenies of *er-105 erl1-2/+ erl2-1/+*, pre-selected for the presence of the *erl1-2* T-DNA insertion, were grown to maturity. This population segregated seven extremely dwarf and sterile plants, consistent with the expected 8.3% ratio for the *er-105 erl1-2 erl2-1* triple mutant (dwarf plants/total=7/100; χ^2=0.221, *P*=0.637). Seventeen additional plants from this population were completely sterile and produced no seeds. However, unlike the triple *er*-family mutants, they did not exhibit severe dwarfism, disrupted phyllotaxis or floral organ patterning defects. A reciprocal cross-pollination with wild type revealed that these plants were female sterile (data not shown).

To determine the genetic basis for this novel phenotype, we next analyzed the genotypes of all 100 plants in this population. All seventeen female-sterile, non-dwarf plants were homozygous for *er-105* and *erl1-2* and heterozygous for *erl2-1* (i.e. *er-105 erl1-2 erl2-1/+*) (Fig. 1E). This was highly consistent with the expected ratio of 16.7% for this population (χ^2=0.006, *P*=0.936). Unlike *er-105 erl1-2 erl2-1/+*, the *er-105 erl1-2/+ erl2-1* plants were fully fertile (Fig. 1F). Reintroduction of functional copies of *ER*, *ERL1* and *ERL2* into respective loss-of-function mutants confirmed these data (see Table S1 in the supplementary material). The results indicate that, in the absence of *ER* and *ERL1*, *ERL2* is haploinsufficient for female fertility, whereas *ERL1* is haplosufficient in the absence of *ER* and *ERL2*. By contrast, the lack of defects in floral morphology (see Fig. S1 in the supplementary material) and phyllotaxis indicate that a single copy of *ERL2* is sufficient for inflorescence elongation and floral patterning.

Slight increase in *ERL1* activity is sufficient to rescue *ERL2* haploinsufficiency

To further investigate the importance of *ERL1* function in female fertility, we generated mutant combinations with two additional *erl1* alleles. The *erl1-1* allele carries a T-DNA insertion 349 bases upstream of the initiation codon and represents a weak allele (Fig. 1I,J). The *erl1-4* allele has a G-to-A substitution at nucleotide position +750. This creates a stop codon at amino acid 61, leading to a premature truncation of the protein prior to the LRR domain (Fig. 1I). Therefore, *erl1-4* is a null allele.

The *er-105 erl1-1 erl2-1*, *er-105 erl1-2 erl2-1* and *er-105 erl1-4 erl2-1* triple-mutant plants were almost indistinguishable from each other (data not shown). Similar to *er-105 erl1-2 er2-1/+* plants (Fig. 1E), *er-105 erl1-4 erl2-1/+* plants were completely female sterile (Fig. 1G). By contrast, *er-105 erl1-1 er2-1/+* plants were fertile and produced viable seed (Fig. 1H). These results demonstrate that a slight increase in *ERL1* activity is sufficient to rescue the haploinsufficiency of *ERL2*. However, because *erl1-1* failed to

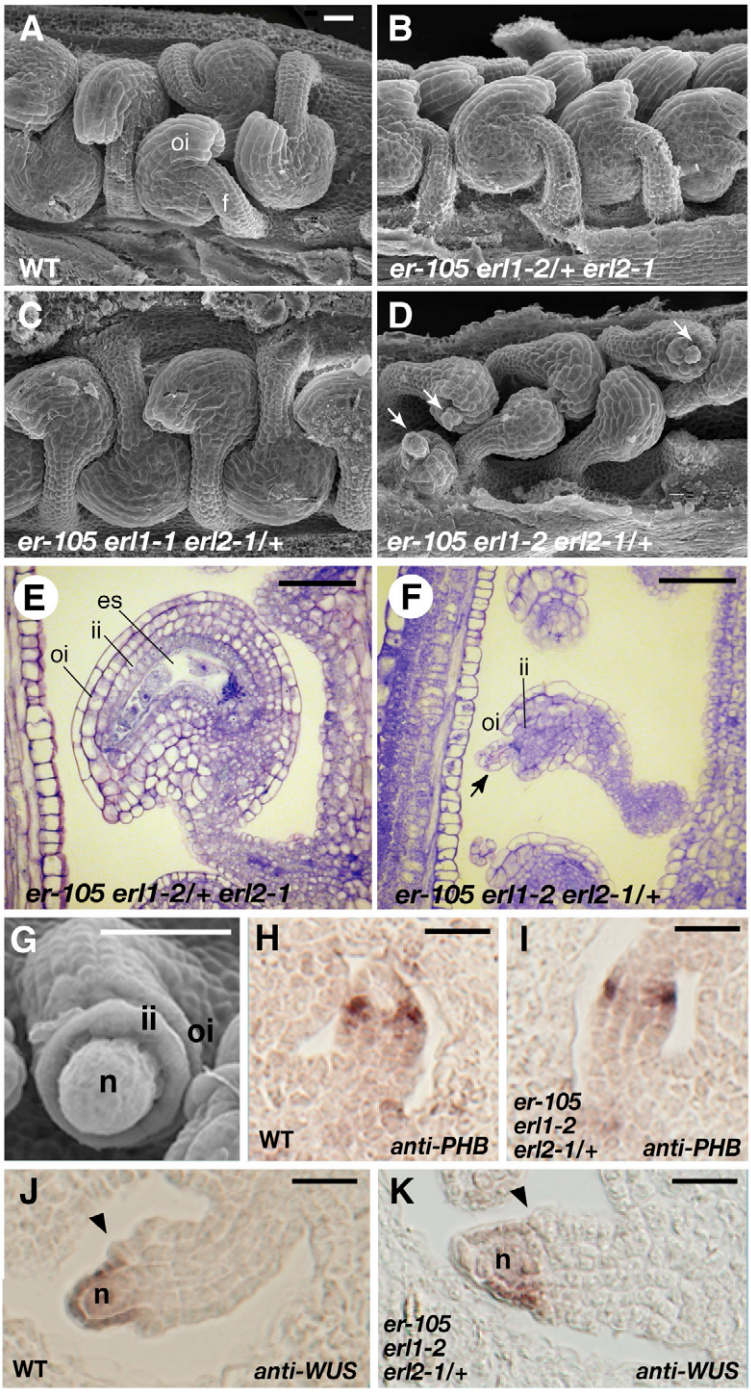

Fig. 2. Phenotypic effects of loss of *er*-family function on ovule development. (**A-D**) Scanning electron micrographs (SEMs) of *Arabidopsis* ovules at anthesis. (A) Wild type; (B) *er-105 erl1-2/+ erl2-1*; (C) *er-105 erl1-1 erl2-1/+*; (D) *er-105 erl1-2 erl2-1/+*. In *er-105 erl1-2 erl2-1/+*, both inner and outer integuments are shorter leaving the nucellus exposed (arrows). (**E**,**F**) Sagittal sections through the gametophyte of a *er-105 erl1-2/+ erl2-1* (E) and *er-105 erl1-2 erl2-1/+* (F) ovule at anthesis. In the *er-105 erl1-2 erl2-1/+* mutant, the gametophyte has degenerated into a mass of small cells. (**G**) SEM of a developing *er-105 erl1-2 erl2-1/+* stage 2-I ovule. Both the inner and outer integument initiate as smooth rings at the base of the nucellus, with the outer integument initiating asymmetrically as in wild type. (**H-K**) In situ hybridization for (H,I) *PHB* and (J,K) *WUS* expression. No difference in *PHB* or *WUS* expression is detected in mutant ovules, indicating normal regional specification. No signal was detected with *PHB* or *WUS* sense probe. f, funiculus; es, embryo sac; ii, inner integument; oi, outer integument; n, nucellus. Scale bars: 20 μm.

promote organ growth, proper floral patterning or fertility in the absence of *ER* and *ERL2*, the results highlight a strict ER-family signaling threshold required to promote female fertility.

Haploinsufficiency of *ERL2* confers aberrant ovule growth and abortion of embryo sac development

To gain insight into the developmental basis of *er-105 erl1-2 erl2-1/+* female sterility, we examined the morphology of mature ovules (stage 13 flowers, anthesis) (Smyth et al., 1990) (Fig. 2). Similar to wild type, *er-105 erl1-2/+ erl2-1* exhibited typical amphitropic ovule morphology (Fig. 2A,B,E). Ovules of *er-105 erl1-1 erl2-1/+* were fertile, but had slightly shorter integuments than wild type, resulting in the micropyle resting slightly away from the funiculus (Fig. 2C). By contrast, the mature ovules of *er-105 erl1-2 erl2-1/+* displayed aberrant morphology. Growth of both inner and outer integuments as well as the funiculus was dramatically compromised, leading to small, stunted ovules that often had an exposed nucellus (Fig. 2D,F). The embryo sac of mature *er-105 erl1-2 erl2-1/+* ovules was absent and replaced by a disorganized mass of small cells (Fig. 2F).

Initiation and polarity of integuments was not disrupted in *er-105 erl1-2 erl2-1/+* (Fig. 2G). To determine whether integument initiation was defined normally, we used *WUS* and *PHB* as a nucellar regional marker and adaxial marker, respectively (Fig. 2H-K). *WUS* is expressed exclusively in the nucellus of wild-type ovules and promotes integument initiation in the chalazal region proximal to its expression domain (Groß-Hardt et al., 2002), whereas *PHB* expression marks the inner integument (Sieber et al., 2004). No alteration in *WUS* or *PHB* expression was detected between wild type and *er-105 erl1-2 erl2-1/+*. These data suggest that loss of ER-family signaling does not disrupt regional domain specification or radial patterning.

Integument outgrowth is compromised in *er-105 erl1-2 erl2-1/+* mutants

To determine the onset of developmental defects, wild-type and *er-105 erl1-2 erl2-1/+* ovules were examined at sequential developmental stages (Fig. 3) (Schneitz et al., 1995). Early ovule initiation and patterning were normal in *er-105 erl1-2 erl2-1/+*, consistent with the normal *PHB* and *WUS* expression patterns (Fig. 2I,K). Similar to wild type, ovule primordia initiated and elongated from the placental wall (stage 1-II; Fig. 3A,E,I). At stage 2-II to 2-V, outer and inner integument primordia arose from the chalaza and grew toward the nucellus (Fig. 3B,F,J). However, starting at stage 3-I, the cells of *er-105 erl1-2 erl2-1/+* outer integuments had a more disorganized appearance than wild type (Fig. 3C,G,K). Enlargement of the megaspore mother cell (MMC) and tetrad formation proceeded as in wild type within the nucellus of *er-105 erl1-2 erl2-1/+* ovules (Fig. 3I,M). However, mutant ovules arrested at a two-nucleate embryo sac (Fig. 3N). We never observed *er-105 erl1-2 erl2-1/+* embryo sacs beyond this two-nucleate stage. Based on our observations, we conclude that progression of integument growth in the absence of

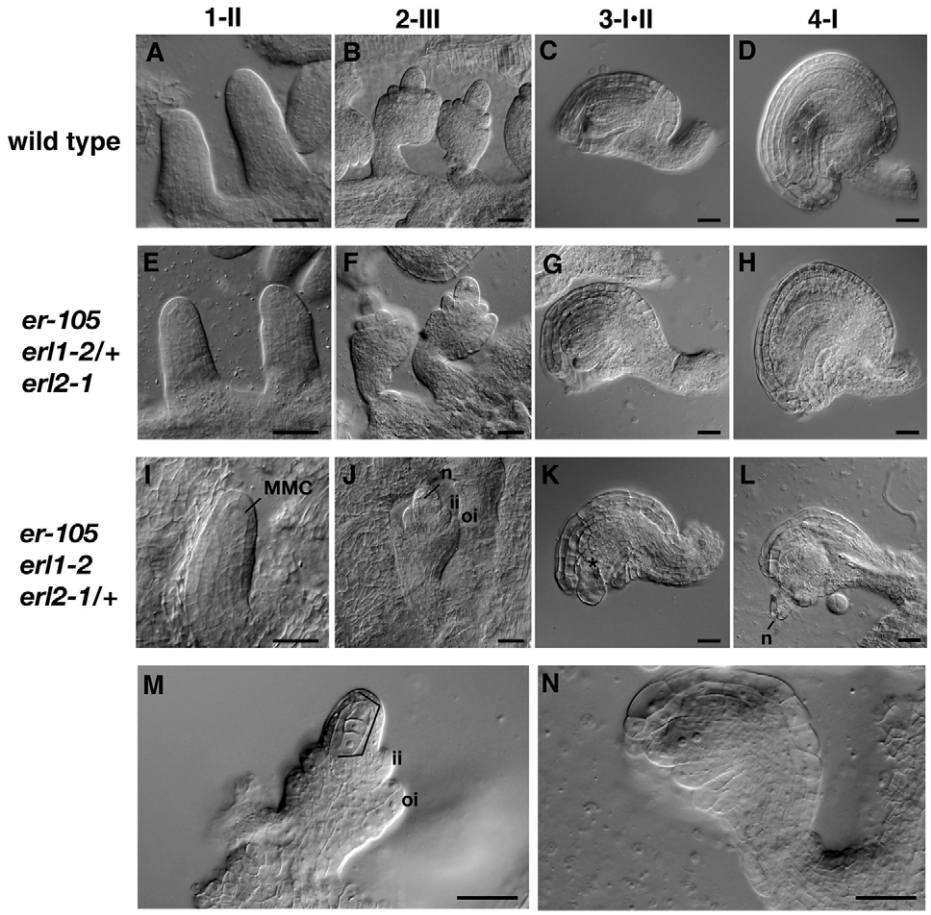

Fig. 3. Developmental series of ovule development in wild-type, *er-105 erl1-2/+ erl2-1* and *er-105 erl1-2 erl2-1/+ Arabidopsis*. (**A-L**) DIC images of ovules at stages: 1-II (A,E,I); 2-III (B,F,J); 3-I II (C,G,K) and 4-I (D,H,L). Differences in development are seen at stage 3-I-II (C,G,K). Asymmetric growth of the outer integument occurs in all genotypes; however, *er-105 erl1-2 erl2-1/+* integuments appear less organized and gametophyte development has ceased (K). By anthesis (D,H,L), the integuments of *er-105 erl1-2 erl2-1/+* are short resulting in the nucellus protruding from the integuments (L). By contrast, the *er-105 erl1-2/+ erl2-1* ovule has nearly normal appearance, with a very subtle phenotype (H). (**M**,**N**) *er-105 erl1-2 erl2-1/+* ovule at stage 2-V with tetrad (M, bracket) and stage 3-II (N) showing two-nuclear gametophyte. MMC, megaspore mother cell; n, nucleus; ii, inner integument; oi, outer integument. Scale bars: 20 μm.

ER is dependent on *ERL1* and *2* in a dosage-dependent manner. At a minimum, *ERL1* in a heterozygous state or *ERL2* in a homozygous state is required.

Reduced cell numbers in *er-105 erl1-2 erl2-1/+* mutants lead to reduced integument size

Change in organ size reflects an alteration in cell size, cell number, or both. To understand the mechanism underlying the phenotype of *er-105 erl1-2 erl2-1/+* ovules, we examined the size and number of cells in developing ovule integuments and compared them with wild type. In wild type, integument cells at the micropylar end were much more elongated than those at the chalazal end (Fig. 2E). The *er erl1 erl2/+* ovules appeared to lack this characteristic polar elongation of integument cells (Fig. 2F). This made the outer integument cells of *er-105 erl1-2 erl2-1/+* ovules less organized and slightly more uniform in length than wild type. However, no significant difference in outer integument cell size area was found between wild-type and mutant ovules (Fig. 4A-C).

We next assessed the possibility of endoreduplication in mutant integument cells by observing the nuclear size using 4′,6-diamidino-2-phenylindole (DAPI). Endoreduplication is the repetitive duplication of chromosomal DNA without mitosis or cytokinesis, resulting in an increase in cell ploidy level (Kondorosi et al., 2000). In plants, a positive correlation between ploidy level and cell size has been observed (Kondorosi et al., 2000; Melaragno et al., 1993). No qualitative difference in the size (area) of nuclei between wild-type and *er-105 erl1-2 erl2-1/+* outer integument cells was observed (see Fig. S2 in the supplementary material), consistent with the absence of a cell size difference between wild-type and mutant integuments.

To investigate whether *er-105 erl1-2 erl2-1/+* ovule integument defects were due to a decrease in cell division, we quantified the number of cells contributing to the epidermis at stage 1-II and to the outer integument at three subsequent stages (see Materials and methods). At stages 1-II and 2-II, no difference in cell number was observed between *er*-family combination mutants and wild type (Fig. 4D). However, *er-105 erl1-2 erl2-1/+* outer integuments had significantly fewer cells per outer integument than wild type from stage 3-III (31% reduction) to maturity (57% reduction). A similar trend was observed for *er-105 erl1-2/+ erl2-1* (15% reduction) and *er erl1-1 erl2-1/+* (30% reduction) ovules, which had an intermediate number of integument cells between that of wild type and *er-105 erl1-2 erl2-1/+* at maturity (Fig. 4D). Together, these data provide evidence that a reduction in cell division is responsible for the abnormal integument morphology of *er-105 erl1-2 erl2-1/+* ovules, and that the number of cell divisions is sensitive to the dosage of *ERL1*.

Specific misregulation of cell-cycle regulators is associated with the arrested ovule development in *er-105 erl1-2 erl2-1/+* mutants

Because cell divisions were reduced in *er-105 erl1-2 erl2-1/+* ovules, we examined the expression of cell-cycle-regulatory genes to determine if their transcript accumulation is altered in *er-105 erl1-2 erl2-1/+* ovules. The cell cycle is regulated at multiple points by cyclin-dependent kinases (CDKs) that form complexes with appropriate cyclins (De Veylder et al., 2003; Dewitte and Murray, 2003). Plants have a large number of core cell-cycle genes including plant specific B-type CDKs that are regulated at the transcriptional

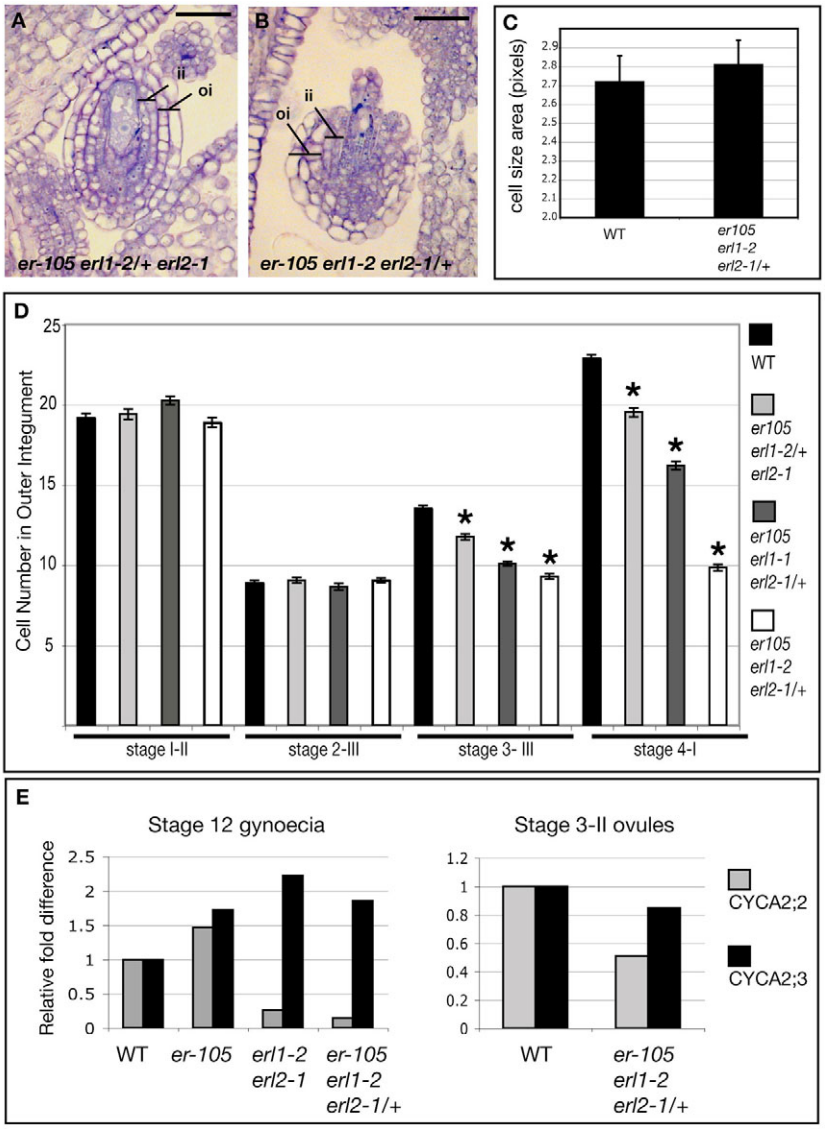

Fig. 4. *ERL2* is haploinsufficient to maintain integument growth. (**A**,**B**) Transverse (horizontal) sections of *Arabidopsis* ovules at anthesis. (A) *er-105 erl1-2/+ erl2-1* has a fully encased and developed embryo sac. (B) *er-105 erl1-2 erl2-1/+* ovule has shorter integuments, protruding nucellus with no observable embryo sac. (**C**) Mean cell area (±s.e.m.) of the outer integument cells of wild type and *er-105 erl1-2 erl2-1/+* (n=25, Student's t-test, P=0.331). (**D**) Cell number (±s.e.m.) in epidermis of ovules (stage 1-II) and the outer layer of the outer integument (stage 2-III, 3-III and 4-I) of wild-type and *er*-family mutant ovules at the indicated stages (n=25). Asterisks indicate a significant difference from the respective wild type within each stage using Student's t-test (P=0.01). At stage 3-III, a decrease in the number of cells in the outer integument is detected between wild type and *er*-family mutants. By stage 4-II, the number of cells in the outer integument is dramatically reduced compared with wild type. (**E**) Real-time RT-PCR analysis of selected cyclins in stage 12 carpels (left) and stage 3-II ovules (right). Loss of ER-family function results in a disruption of cyclin gene expression. Scale bars: 20 μm.

level (De Veylder et al., 2003). Plant cyclin genes can be divided into four groups (A, B, D and H). The evolution of three A-type subclasses (A1, A2 and A3), compared with only one in animals, has led to the idea that A-type cyclins might fulfil plant-specific roles (Caubet-Gigot, 2000; Dewitte and Murray, 2003).

To detect alterations in expression levels of cell-cycle regulatory genes, we performed RT-PCR analysis on RNA from stage 12 carpels (see Fig. S3 in the supplementary material). According to Schneitz et al. (Schneitz et al., 1995), this stage of carpel corresponds to the point in ovule development when we observed noticeable changes in integument morphology between *er-105 erl1-2 erl2-1*/+ and wild type. Most of the B-type CDKs and cyclin A, B and D genes did not show a dramatic change in transcript abundance in ER-family loss-of-function mutants. However, *CYCA2;2* showed a pronounced decrease in expression in *er-105 erl1-2 erl2-1*/+ (see Fig. S3 in the supplementary material; data not shown). We next quantified the relative decrease in *CYCA2;2* transcripts using real-time PCR. We found that *CYCA2;2* consistently shows a significant decrease in expression after loss of *ER*-family function in both carpels and individual ovules (Fig. 4E). Conversely, *CYCA2;3* had the opposite trend, showing increased transcript accumulation after *ER*-family loss-of-function, perhaps owing to compensation (Fig. 4E). The results suggest that reduced levels of *ER*-family gene function may impact cell division through disruption of specific cell-cycle-regulatory gene expression.

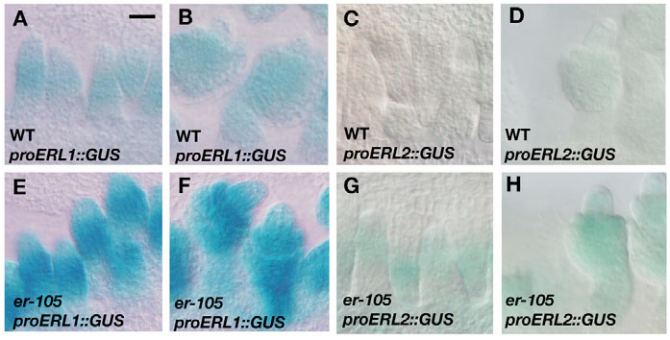

Fig. 5. The ER family of LRR-RLKs are expressed in ovules throughout development. (**A**,**B**) *proERL1::GUS* expression in wild-type *Arabidopsis*. (**C**,**D**) *proERL2::GUS* expression in wild type. (**E**,**F**) *proERL1::GUS* expression in *er-105*. (**G**,**H**) *proERL2::GUS* expression in *er-105*. *ERL1* and *ERL2* promoter activity is higher in the *er-105* background than in wild type. Scale bar: 20 μm.

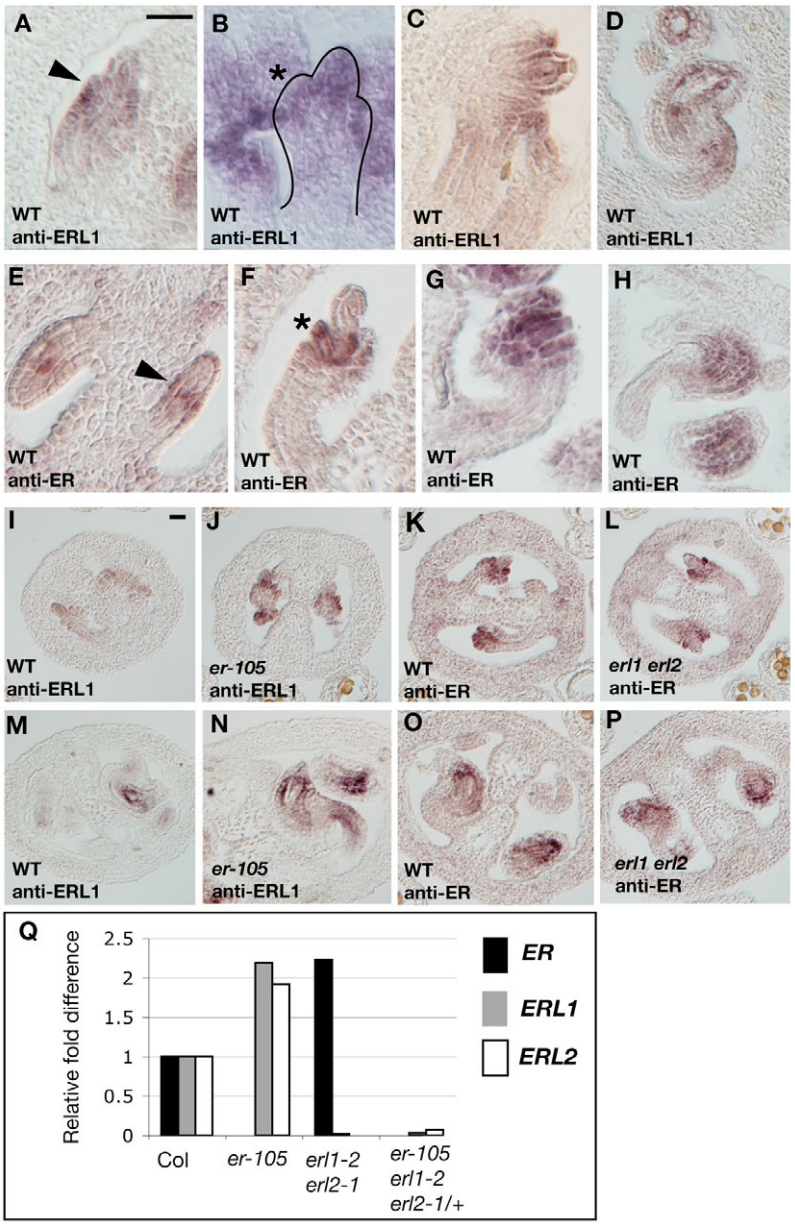

Fig. 6. *ERL1* and *ER* expression patterns. (**A-H**) In situ hybridization in wild-type *Arabidopsis* using an *ERL1* (A-D) or *ER* (E-H) antisense probe. Both show broad expression in ovules with increased signal intensity in the chalazal region (A,E, arrowheads) and developing integuments (B,F, asterisks). Ovule is outlined in B. (D,H) Signal is still visible at maturity. (**I-P**) Comparison of *ERL1* (I,J,M,N) or *ER* (K,L,O,P) mRNA accumulation in wild type and ER-family mutants examined by in situ hybridization. (**Q**) Real-time RT-PCR analysis of *ER*, *ERL1* and *ERL2* in stage 12 carpels of wild type and *ER*-family mutants. Transcript abundance of *ER*, *ERL1* and *ERL2* are higher in the absence of the other family members. Scale bars: 20 μm.

Alternatively, altered levels of these cyclin genes could be the consequence of reduced cell division produced by a yet unknown mechanism.

ERL1 and *ERL2* are expressed in ovule primordia and developing integuments

To determine the expression pattern of the *ER* family during ovule development, we first observed their promoter activity using reporter β-glucuronidase (GUS) fusion constructs (Fig. 5) (Shpak et al., 2004). *ERL1* and *ERL2* promoter activity was first detected in the placental wall prior to ovule primordia initiation (data not shown). They became broadly active in ovules with a slight increase in activity in the central chalazal region (Fig. 5A-D). In mature ovules, faint GUS expression was restricted to the funiculus (data not shown). Interestingly, *proERL1::GUS* was notably stronger in the *er-105* background than in wild type (Fig. 5E,F).

Because integument growth was sensitive to the dosage of *ERL1* and because the promoter activity of *ERL1* and *ERL2* are similar, we focused our analysis of expression overlap on *ER* and *ERL1*. We analyzed the mRNA expression patterns of *ER* and *ERL1* by in situ hybridization (Fig. 6). In reproductive structures, *ERL1* transcripts were detected in floral meristems and primordia (see Fig. S4 in the supplementary material). During ovule development, *ERL1* transcripts were detected throughout ovule primordia from initiation to stage 3-II, with increased hybridization intensity in the chalazal region and developing integuments (Fig. 6A-C). At maturity, *ERL1* hybridization signal was still detectable in the integuments and funiculus (Fig. 6D).

Expression of *ER* was observed in floral meristems as well as the carpel wall and developing petals (see Fig. S4 in the supplementary material). Similar to *ERL1*, *ER* transcripts were detected broadly in the developing ovule, with more intense signal in the chalazal region and developing integuments (Fig. 6E-G). *ER* expression lessened later in development, but was still detectable in the carpel and ovule integuments at maturity (Fig. 6H). As the probes for *ER* and *ERL1* did not cross-hybridize with each other (see Fig. S4 in the supplementary material), our results suggest that overlapping expression patterns of *ER* and *ERL1* account for their redundant roles in ovule development.

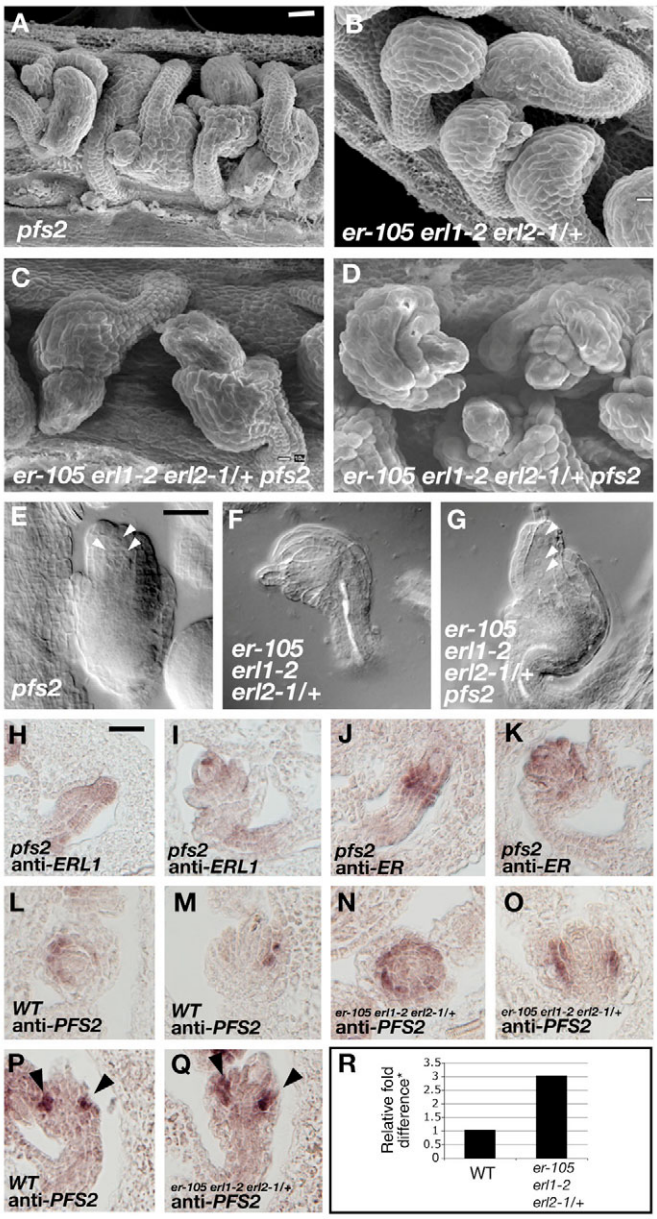

Fig. 7. Genetic interactions of *ER-family* genes with *PFS2*. (**A-D**) SEMs of mature *Arabidopsis* ovules. (A) *pfs2-1* ovules have aberrant integument development. (B) *er-105 erl1-2 erl2-1/+* ovules. (C,D) *er-105 erl1-2 erl2-1/+ pfs2-1* mutant ovules have variability in integument development with reduced growth of the outer integument and some bifurcation of developing integuments. (**E-G**) DIC images of mature ovules. (E) *pfs2-1* ovules have some partially developed embryo sacs. (F) *er-105 erl1-2 erl2-1/+* has a penetrant phenotype of a small mass of cells in place of the embryo sac. (G) *er-105 erl1-2 erl2-1/+ pfs2-1* mutant ovules display variability in embryo sac development similar to the *pfs2-1* single mutant. Embryo sac nuclei are indicated by white arrowheads. (**H-K**) In situ hybridization in the *pfs2-1* mutant using *ERL1* (H,I) and *ER* (J,K) antisense probes. (**L**,**M**) In situ hybridization in wild type using a *PFS2* antisense probe. (**N**,**O**) In situ hybridization in *er-105 erl1-2 erl2-1/+* using a *PFS2* antisense probe. (**P**,**Q**) Extended exposure of *PFS2* antisense probe in wild type and *er-105 erl1-2 erl2-1/+*. Intense signal was observed in the inner integuments (arrowheads). No signal was detected with sense probes for *ERL1*, *ER* or *PFS2*. Scale bars: 20 μm. (**R**) Real-time RT-PCR analysis of *PFS2* expression in stage 3-II ovules, given as fold-difference relative to wild type. *, Raw data collected as *PFS2* transcript abundance relative to *ACTIN 2* (wild type versus *er-105 erl1-2 erl2-1/+*. Experiment 1: 0.205±0.04 versus 0.351±0.02; Student's *t*-test *P*=0.03; 1.72 fold increase in *er-105 erl1-2 erl2-1/+*. Experiment 2: 0.141±0.003 versus 0.603±0.04; Student's *t*-test *P*=0.001; 4.2 fold increase in *er-105 erl1-2 erl2-1/+*).

Unequal dosage compensation among *ER*-family genes

Given the overlapping expression patterns of *ER*-family genes in the ovule and their ability to functionally substitute for one another (Shpak et al., 2004), we tested whether loss of specific *ER*-family gene function would lead to changes in expression of the other family members. To assess changes in transcript abundance, quantitative real-time RT-PCR analysis was performed on RNA from stage 12 carpels (Fig. 6Q). An increase in both *ERL1* and *ERL2* transcripts was observed in the *er-105* background as compared with wild type and, reciprocally, the accumulation of *ER* transcripts was higher in the *erl1 erl2* mutant background. In situ hybridization determined that the spatial expression patterns of *ER* and *ERL1* were not disrupted in the *er-105* and *erl1 erl2* mutant backgrounds (Fig. 6I-P), respectively.

Taken together, the results suggest that transcriptional upregulation occurs in the absence of *ER*-family members, allowing each family member to functionally compensate for each other. This is consistent with the findings of Shpak et al. (Shpak et al., 2004) that ER-family members are able to substitute for each other if their temporal and spatial expression patterns overlap. Fertility in the null *er* single mutant or *erl1 erl2* double mutant might require dosage compensation by the remaining family members to maintain signaling above a required threshold. This threshold is not met in the *er-105 erl1 erl2/+* mutant, resulting in the arrest of integument growth.

Interaction of *pfs2* with *er erl1-2 erl2-1/+*

PFS2, a *WUS*-related homeobox gene also known as *WOX6*, affects ovule patterning and regulates integument cell proliferation and gametophyte differentiation (Park et al., 2004; Park et al., 2005). It has been well-documented that the competing actions of the transcription factor WUS, and the CLAVATA (CLV) LRR-RLK signaling pathway, maintain meristem size in *Arabidopsis* (Brand et al., 2000). Numerous WOX genes display region-specific expression, but relatively little is known about their regulation (Haecker et al., 2004). To investigate whether a mechanism including *PFS2* and *ER* signaling directs integument size during ovule development, we produced the combination mutant *er-105 erl1-2 erl2-1/+ pfs2-1* and characterized the phenotype.

The *pfs2-1*-null mutation causes the production of ovules with similar characteristics to *er-105 erl1-2 erl2-1/+*. *pfs2-1* ovules have aberrant integument growth after initiation and embryo sac arrest (Park et al., 2004) (Fig. 7A). However, growth defects are variable in *pfs2-1* mutants: some ovules complete various stages of embryo sac development and a low percentage of viable seed are produced (Park et al., 2005). Similar to *pfs2-1* alone, we observed a variable degree of integument development in the *er-105 erl1-2 erl2-1/+ pfs2-1* mutant (Fig. 7C,D). The phenotype ranged from an outer integument that covered the inner integument to a near absence of the outer integument. In addition, subtle changes in integument

development were observed including lobing of the outer integument during development (Fig. 7C,D). Such variability in integument growth was not observed in *er-105 erl1-2 erl2-1/+*, in which the phenotype showed little variation (Fig. 7B). Surprisingly, some ovules of *er-105 erl1-2 erl2-1/+ pfs2-1* developed beyond the two-celled nuclei stage typical of *er-105 erl1-2 erl2-1/+* ovules, although no viable seed could be collected from these plants (Fig. 7E-G). Therefore, the loss of *PFS2* function partially rescues the *er-105 erl1-2 erl2-1/+* ovule defects.

Because *pfs2-1* ovules show aberrant integument growth, we performed in situ hybridization using *ER* and *ERL1* probes in the *pfs2-1* ovules to determine whether loss of ER-family signaling contributed to the abnormal integument phenotype of *pfs2-1* ovules (Fig. 7H-K). Loss or change in expression domain of *ER* or *ERL1* was not detected in the *pfs2-1* mutant, suggesting that the required threshold of ER-signaling is met in the *pfs2-1* mutant.

The phenotypic rescue of *er-105 erl1-2 erl2-1/+* ovules by additional *pfs2* mutation implies that it is advantageous not to have *PFS2* under the sub-threshold level of ER-family signaling. To test whether the *er-105 erl1-2 erl2-1/+* phenotype was due in part to misexpression of *PFS2*, we performed in situ hybridization using a *PFS2* probe (Fig. 7L-O). *PFS2* expression was detected broadly in developing carpels and initiating ovule primordia (data not shown) with strong expression in the inner integument during initiation and growth (Fig. 7L-O). The expression domain of *PFS2* was not altered in the *er-105 erl1-2 erl2-1/+* ovules (Fig. 7P,Q), indicating that the gametophytic defects in *er-105 erl1-2 erl2-1/+* are not due to *PFS2* misexpression. However, quantitative real-time RT-PCR detected an increase in *PFS2* transcript abundance in *er-105 erl1-2 erl2-1/+* stage 3-II ovules compared with wild type, indicating a potential inhibitory role for the ER family in *PFS2* expression. Phenotypic rescue of *er-105 erl1-2 erl2-1/+* by the addition of the *pfs2* mutation suggests that ovule development requires a proper balance of both *ER* family and *PFS2* function.

DISCUSSION

Unequal functional redundancy among the ER-family LRR-RLKs

Gene duplication is a common occurrence and has led to the production of numerous gene families in *Arabidopsis*, one of the largest being the RLK-coding gene family, which has over 600 members (Shiu and Bleecker, 2001; Vision et al., 2000). Following a gene duplication event, decreased selection pressure on one of the gene copies can produce proteins with novel function or expression resulting in partial redundancy among gene family members (Hardtke et al., 2004). If the shared function of duplicated genes becomes unequally distributed between gene copies, unequal redundancy among the gene family members may result, as described for the *ER* family, where both *erl1* and *erl2* confer no growth phenotype but enhance the *er* growth defects in a unique manner (Kempin et al., 1995; Shpak et al., 2004). In many cases, unequal redundancy is produced by differences in the expression level or expression patterns between gene copies, where the duplicated gene(s) may have redundant function with the ancestral gene, but the expression might be lower or restricted. A good example is the three *Arabidopsis* brassinosteroid receptor genes. The major receptor, *BRI1*, is broadly expressed at high levels, whereas expression of *BRL2* and *BRL3* is restricted to vasculature (Cano-Delgado et al., 2004). Successive loss of family members enhances the phenotype of the ancestral gene and a true null phenotype is observed only in the absence of the entire family as has been shown for *ER*, *ERL1* and *ERL2* (Shpak et al., 2004).

Our study uncovered unequal contributions and dosage compensation among gene family members with overlapping expression patterns. The most significant difference between *er-105 erl1-2/+ erl2-1* and *er-105 erl1-2 erl2-1/+* plants is the loss of female fertility owing to reduced cell division and outgrowth of the integuments in *er-105 erl1-2 erl2-1/+*. The expression pattern for all three family members overlaps in the distal, central and proximal regions, consistent with all three regions being reduced when successive family members are removed. An *erl1-2 erl2-1* double or *er* single mutant shows no obvious defects in integument development, indicating that the upregulation of *ER* or *ERL1* and *2* in these backgrounds can maintain expression above the threshold necessary to direct integument development (Fig. 6Q). However, as successive family members are lost, low levels of *ERL2* are insufficient to maintain signaling, and integument growth is compromised. Consistent with this dosage-dependence model, the ovules of *er-105 erl1-2 erl2-1/+* are significantly larger and more developed than those of the *ER*-family triple mutant (see Fig. S5 in the supplementary material).

ERL2 haploinsufficiency specifically affects cell division of the ovule integuments

The ER-family LRR-RLKs probably maintain cell-cell communication, a reduction of which results in the irregular and reduced cell division during integument outgrowth in *er-105 erl1-2 erl2-1/+* ovules. They do not regulate ovule primordia patterning or integument initiation, as these aspects are not affected even by the complete loss of ER-family function (Fig. 2 and see Fig. S5 in the supplementary material).

Our results suggest that the ER-family RLKs promote cell division after integument initiation through potential regulation of core cell-cycle genes, specifically *CYCA2;2* (Fig. 4). Among over 30 cyclins present in *Arabidopsis*, ten belong to the A-type (Dewitte and Murray, 2003; Vandepoele et al., 2002). Recent studies suggest that *Arabidopsis* cyclin A2 families act as negative regulators of endoreduplication (Burssens et al., 2000; Dewitte and Murray, 2003; Imai et al., 2006; Yu et al., 2003). For example, loss-of-function mutations in *CYCA2;3* led to elevated ploidy levels in mature organs (Imai et al., 2006). Consistently, the dominant, activation-tagged mutation in *INCREASED LEVEL OF POLYPLOIDY1*, a conserved repressor of *CYCA2* transcription, caused an increase in endoreduplication (Yoshizumi et al., 2006). However, cyclin A2 families may also function to regulate mitosis. In *Medicago*, *CYCA2;2* (*MedsaCYCA2;2*) is required for meristem formation or activity but dispensable for endoreduplication (Roudier et al., 2000). Similar to *Medsa;CYCA2;2*, all four *Arabidopsis* cyclin A2 genes show high promoter activity in meristems and young organ primordia (Burssens et al., 2000; Imai et al., 2006). Therefore, they might redundantly control cell division in actively proliferating tissues, where the ER-family signaling pathway is required. Consistent with this hypothesis, flow-cytometric analysis of DNA content in *er-105* suggested possible cell-cycle arrest (Shpak et al., 2003).

All members of the ER family are expressed in overlapping domains in additional areas of the plant including shoot and inflorescence meristems and floral primordia (Shpak et al., 2004). The lack of any visual *er-105 erl1-2 erl2-1/+* phenotype in these tissues could be due to redundancy by other signaling factors that are not expressed in the ovule. Alternatively, ovule integuments might be particularly susceptible to cell-cell signaling disruption. Unlike meristems and developing leaves and floral organs, integuments are solely derived from the L1 layer (Schneitz et al., 1997). Therefore, cell proliferation in integuments is likely to

occur with limited inter cell-layer communication. Such a scenario was suggested for loss-of-function mutants of the RLK gene *ARABIDOPSIS CRINKLY4*, which display localized defects in integument development, despite its expression in a wider variety of tissues (Gifford et al., 2003).

Genetic interaction of *ER*-family genes and PFS2

PFS2 is thought to control ovule primordial patterning by regulating the timing of cellular differentiation (Park et al., 2005). In *pfs2-1*, premature differentiation of the cells contributing to the gametophyte or integument primordia could account for decreased integument length and defects in the embryo sac (Park et al., 2004). The addition of *pfs2-1* to *er-105 erl1-2 erl2-1/+* mutations led to increased variability in both integument and gametophyte development, similar to *pfs2-1* alone, indicating that the *pfs2-1* mutation is epistatic to the *er*-family mutations. One explanation for these results is that the ER-family RLKs and PFS2 both contribute to integument outgrowth through distinct but interrelated mechanisms. The ER family are components of a signaling pathway that sustain organized cell divisions, potentially through the regulation of core cell-cycle genes such as *CYCA2;2*. Without activation of this signaling pathway, integument cells may differentiate before undergoing sufficient cell divisions. *PFS2* might be responsible for maintaining integument cells in a state that allows them to respond to factors required for coordinated cell division. In this scenario, the loss of PFS2 function would be epistatic to the loss of the ER family.

WOX genes generally have a spatially restricted expression pattern (Matsumoto and Okada, 2001). Our in situ hybridization shows that *PFS2* expression is spatially restricted to the inner integument (Fig. 7). Therefore, *PFS2* might be required to properly coordinate the developmental states of the sporophytic integument tissues and gametophytic embryo sac. If so, the loss of *PFS2* uncouples embryo sac development from abrogated integument growth under the sub-threshold level of ER-family signaling, therefore partially rescuing the embryo sac defects in *erecta-105 erl1-2 erl2-1/+* ovules.

In the well-established model of *CLV/WUS* interaction in the shoot meristem, *CLV3* limits the expression of *WUS*, while *WUS* in turn promotes the expression of *CLV3*, causing a feedback loop that maintains a stem cell population (Brand et al., 2000; Clark, 2001; Laux et al., 1996). Our results indicate that the ER family does not spatially restrict PFS2 expression and that factors yet to be identified are likely to be responsible for the limiting *PFS2* expression. However, the ER family might restrict the expression levels of *PFS2*, and elevated expression of *PFS2* might account for the abortion of gametophytes in *er-105 erl1-2 erl2-1/+* ovules. Consistently, embryo sacs of *er-105 erl1-2 erl2-1/+* are filled with a small group of cells, which resembles the phenotype of *PFS2* overexpression described by Park et al. (Park et al., 2005).

Haploinsufficiency refers to a phenotype associated with the inactivation of a single allele leading to a half-normal amount of gene product, which is insufficient to maintain the wild-type phenotype. In this report, we have shown a novel phenotype for successive ER-family loss-of-function; *ERL2* is haploinsufficient in the absence of *ER* and *ERL1* to direct integument growth, but sufficient to drive floral organ growth, elongation and patterning. We further uncovered evidence of dosage compensation within the ER family and their potential regulatory relationships with the WOX-family transcription factor. Our work has identified the specific timing of *ERL1* action during integument cell proliferation, which might provide a biological system to further elucidate the signaling components.

We thank Dr John Bowman for the *erl1-1* enhancer-trap line, Dr Bernard Hauser for *pfs2-1* seeds, Drs Kiyotaka Okada, Mitsuhiro Aida and Masao Tasaka for *PHB* probes, Dr Caroline Josefsson for assistance in RT-PCR analysis of *erl1-1*, Dr Kay Schneitz for advice on the design of the genetic screen and Dr Jessica Messmer-McAbee for commenting on the manuscript. This work was supported by the USDA CREES postdoctoral fellowship to L.J.P. and by the DOE grant (DE-FG02-03ER15448) to K.U.T. The DIC microscopy was supported by the CREST award from Japan Science and Technology Agency to K.U.T.

Supplementary material

Supplementary material for this article is available at
http://dev.biologists.org/cgi/content/full/134/17/3099/DC1

References

Brand, U., Fletcher, J. C., Hobe, M., Meyerowitz, E. M. and Simon, R. (2000). Dependence of stem cell fate in Arabidopsis on a feedback loop regulated by CLV3 activity. *Science* **289**, 617-619.

Burssens, S., Engler, J. A., Beeckman, T., Richard, C., Shaul, O., Ferreira, P., Van Montagu, M. and Inzé, D. (2000). Developmental expression of the *Arabidopsis thaliana* CycA2;1 gene. *Planta* **211**, 623-631.

Cano-Delgado, A., Yin, Y., Yu, C., Vafeados, D., Mora-Garcia, S., Cheng, J., Nam, K. H., Li, J. and Chory, J. (2004). BRL1 and BRL3 are novel brassinosteroid receptors that function in vascular differentiation in Arabidopsis. *Development* **131**, 5341-5351.

Caubet-Gigot, N. (2000). Plant A-type cyclins. *Plant Mol. Biol.* **43**, 659-675.

Clark, S. E. (2001). Cell signaling at the shoot apical meristem. *Nat. Rev. Mol. Cell Biol.* **2**, 276-284.

De Veylder, L., Joubes, L. and Inzé, D. (2003). Plant cell cycle transitions. *Curr. Opin. Plant Biol.* **6**, 536-543.

Dewitte, W. and Murray, J. A. H. (2003). The plant cell cycle. *Annu. Rev. Plant Biol.* **54**, 235-264.

Ehsan, H., Reichheld, J. P., Durfee, T. and Roe, J. L. (2004). TOUSLED kinase activity oscillates during the cell cycle and interacts with chromatin regulators. *Plant Physiol.* **134**, 1488-1499.

Elliott, R. C., Betzner, A. S., Huttner, E., Oakes, M. P., Tucker, W. Q. J., Gerentes, D., Perez, P. and Smyth, D. R. (1996). *AINTEGUMENTA*, an *APETALA2*-like gene of Arabidopsis with pleiotropic roles in ovule development and floral organ growth. *Plant Cell* **8**, 155-168.

Eshed, Y., Baum, S. R., Perea, J. V. and Bowman, J. L. (2001). Establishment of polarity in lateral organ of plants. *Curr. Biol.* **11**, 1251-1260.

Eshed, Y., Izhaki, A., Baum, S. R., Floyd, S. K. and Bowman, J. L. (2004). Asymmetric leaf development and blade expansion in *Arabidopsis* are mediated by KANADI and YABBY activities. *Development* **127**, 725-734.

Gasser, C. S., Broadhvest, J. and Hauser, B. A. (1998). Genetic analysis of ovule development. *Annu. Rev. Plant Physiol. Plant Mol. Biol.* **49**, 1-24.

Gifford, M. L., Dean, S. and Ingram, G. C. (2003). The Arabidopsis ACR4 gene plays a role in cell layer organisation during ovule integument and sepal margin development. *Development* **130**, 4249-4258.

Groß-Hardt, R., Lenhard, M. and Laux, T. (2002). *WUSCHEL* signaling functions in interregional communicaton during Arabidopsis ovule development. *Genes Dev.* **16**, 1129-1138.

Haecker, A., Groß-Hardt, R., Geiges, B., Sarkar, A., Breuninger, H., Herrmann, M. and Laux, T. (2004). Expression dynamics of *WOX* genes mark cell fate decisions during early embryonic patterning in *Arabidopsis thaliana*. *Development* **131**, 657-668.

Hardtke, C. S., Ckurshumova, W., Vidaurre, D. P., Singh, S. A., Stamatiou, G., Tiwari, S. B., Hagenn, G., Guilfoyle, T. J. and Berleth, T. (2004). Overlapping and non-redundant functions of the *Arabidopsis* auxin response factors *MONOPTEROS* and *NONPHOTOTROPIC HYPOCOTYL 4*. *Development* **131**, 1089-1100.

Hauser, B. A., He, J. Q., Park, S. O. and Gasser, C. S. (2000). TSO1 is a novel protein that modulates cytokinesis and cell expansion in *Arabidopsis*. *Development* **127**, 2219-2226.

Imai, K. K., Ohashi, Y., Tsuge, T., Yoshizumi, T., Matsui, M., Oka, A. and Aoyama, T. (2006). The A-type cyclin CYCA2;3 is a key regulator of ploidy levels in *Arabidopsis* Endoreduplication. *Plant Cell* **18**, 382-396.

Kempin, S. A., Savidge, B. and Yanofsky, M. F. (1995). Molecular basis of the cauliflower phenotype in Arabidopsis. *Science* **267**, 522-525.

Kondorosi, E., Roudier, F. and Gendreau, E. (2000). Plant cell size control: growing by ploidy? *Curr. Opin. Plant Biol.* **3**, 488-492.

Lang, J. D., Ray, S. and Ray, A. (1994). sin1, a mutation affecting female fertility in Arabidopsis, interacts with mod1, its recessive modifier. *Genetics* **137**, 1101-1110.

Laux, T., Mayer, K. F., Berger, J. and Jurgens, G. (1996). The *WUSCHEL* gene is required for shoot and floral meristem integrity in *Arabidopsis*. *Development* **122**, 87-96.

Matsumoto, N. and Okada, K. (2001). A homeobox gene, *PRESSED FLOWER*, regulates lateral axis-dependent development of Arabidopsis flowers. *Genes Dev.* **15**, 3355-3364.

McAbee, J. M., Hill, T. A., Skinner, D. J., Izhaki, A., Hauser, B. A., Meister, R. J., Reddy, G. V., Meyerowitz, E. M., Bowman, J. L. and Gasser, C. S. (2006). ABERRANT TESTA SHAPE encodes a KANADI family member, linking polarity determination to separation and growth of Arabidopsis integuments. *Plant J.* **46**, 522-531.

Melaragno, J. E., Mehrotra, B. and Coleman, A. W. (1993). Relationship between endopolyploidy and cell size in epidermal tissue of Arabidopsis. *Plant Cell* **5**, 1661-1668.

Mizukami, Y. (2001). A matter of size: developmental control of organ size in plants. *Curr. Opin. Plant Biol.* **4**, 533-539.

Park, S. O., Hwang, S. and Hauser, B. A. (2004). The phenotype of *Arabidopsis* ovule mutants mimics the morphology of primitive seed plants. *Proc. R. Soc. Lond. B Biol. Sci.* **271**, 311-316.

Park, S. O., Zheng, Z., Oppenheimer, D. G. and Hauser, B. A. (2005). The PRETTY FEW SEEDS2 gene encodes an Arabidopsis homeodomain protein that regulates ovule development. *Development* **132**, 841-849.

Potter, C. J. and Xu, T. (2001). Mechanisms of size control. *Curr. Opin. Genet. Dev.* **11**, 279-286.

Roudier, F., Fedoova, E., Gyorgyey, J., Feher, A., Brown, S., Kondorosi, A. and Kondorosi, E. (2000). Cell cycle function of a *Medicago sativa* A2-type cyclin interating with PSTAIRE-type cylin-dependent kinase and retinoblastoma protein. *Plant J.* **23**, 73-83.

Schneitz, K., Hülskamp, M. and Pruitt, R. E. (1995). Wild-type development in *Arabidopsis thaliana*: a light microscope study of cleared whole-mount tissue. *Plant J.* **7**, 731-749.

Schneitz, K., Hülskamp, M., Kopczak, S. and Pruitt, R. E. (1997). Dissection of sexual organ ontogenesis: a genetic analysis of ovule development in *Arabidopsis thaliana*. *Development* **124**, 1367-1376.

Schneitz, K., Baker, S. C., Gasser, C. S. and Redweik, A. (1998). Pattern formation and growth during floral organogenesis: *HUELLENLOS* and *AINTEGUMENTA* are required for the formation of the proximal region of the ovule primordium in *Arabidopsis thaliana*. *Development* **125**, 2555-2563.

Sessions, A., Weigel, D. and Yanofsky, M. F. (1999). The *Arabidopsis thaliana MERISTEM LAYER 1* promoter specifies epidermal expression in meristems and young primordia. *Plant J.* **20**, 259-263.

Shiu, S. H. and Bleecker, A. B. (2001). Receptor-like kinases from Arabidopsis form a monophyletic gene family related to animal receptor kinases. *Proc. Natl. Acad. Sci. USA* **98**, 10763-10768.

Shpak, E. D., Lakeman, M. B. and Torii, K. U. (2003). Dominant-negative receptor uncovers redundancy in the Arabidopsis ERECTA leucine-rich repeat receptor-like kinase signaling pathway that regulates organ shape. *Plant Cell* **15**, 1095-1110.

Shpak, E. D., Berthiaume, C. T., Hill, E. J. and Torii, K. U. (2004). Synergistic interaction of three ERECTA-family receptor-like kinases controls Arabidopsis organ growth and flower development by promoting cell proliferation. *Development* **131**, 1491-1501.

Sieber, P., Gheyselinck, J., Gross-Hardt, R., Laux, T., Gossniklaus, U. and Schneitz, K. (2004). Pattern formation during early ovule development in Arabidopsis thaliana. *Dev. Biol.* **273**, 321-334.

Skinner, D. J., Hill, T. A. and Gasser, C. S. (2004). Regulation of ovule development. *Plant Cell* **16**, S32-S45.

Smyth, D. R., Bowman, J. L. and Meyerowitz, E. M. (1990). Early flower development in Arabidopsis. *Plant Cell* **2**, 755-767.

Torii, K. U. (2004). Leucine-rich repeat receptor kinases in plants: structure, function and signal transduction. *Int. Rev. Cytol.* **234**, 1-46.

Torii, K. U., Mitsukawa, N., Oosumi, T., Matsuura, Y., Yokoyama, R., Whittier, R. F. and Komeda, Y. (1996). The Arabidopsis *ERECTA* gene encodes a putative receptor protein kinase with extracellular leucine-rich repeats. *Plant Cell* **8**, 735-746.

Vandepoele, K., Raes, J., De Veylder, L., Rouze, P., Rombauts, S. and Inze, D. (2002). Genome-wide analysis of core cell cycle genes in Arabidopsis. *Plant Cell* **14**, 903-913.

Villanueva, J. M., Broadhvest, J., Hauser, B. A., Meister, R. J., Schneitz, K. and Gasser, C. S. (1999). INNER NO OUTER regulates abaxial-adaxial patterning in Arabidopsis ovules. *Genes Dev.* **13**, 3160-3169.

Vision, T. J., Rown, D. G. and Tanksley, S. D. (2000). The origins of genomic duplications in Arabidopsis. *Science* **290**, 2114-2117.

Yoshizumi, T., Tsumoto, Y., Takigushi, T., Nagata, N., Yamamoto, Y. Y., Kawashima, M., Ichikawa, T., Nakaawa, M., Yamamoto, N. and Matsui, M. (2006). INCREASED LEVEL OF POLYPLOIDY1, a conserved repressor of *CYCLINA2* transcription, controls endoreduplication in *Arabidopsis*. *Plant Cell* **18**, 2452-2468.

Yu, Y., Steinmetz, A., Peng, C.-Y., Yee, A. S. and Piwnica-Worms, H. (2003). The tobacco A-type *Nicta;CYCA3;2*, at the nexus of cell division and differentiation. *Plant Cell* **15**, 2763-2777.

Table S1. Reintroduction of functional alleles of *ERECTA*-family genes

Cross	Functional alleles reintroduced	Number of plants F1	Expected phenotype sterile/fertile	Observed phenotype sterile/fertile	Segregation ratio
er-105 erl1-2 × *er-105 erl1-2/+ erl2-1*	*ERL2*	82	41/41	43/39[‡]	1:1*
er-105 erl2-1 × *er-105 erl1-2/+ erl2-1/+*	*ERL1*	52	0/52	0/52	0:1[†]
erl1-2 erl2-1 × *er-105 erl1-2/+ erl2-1*	*ER*	178	0/178	0/178	0:1[†]

*χ^2 test, P=0.65868742, confirming that *ERL2* is haploinsufficient in the absence of *ER* and *ERL1*.

[†]Confirming that *ERL1* and *ER* are haplosufficient in the absence of *ER* and *ERL2*, and *ERL1* and *ERL2*, respectively.

[‡]All 43 sterile plants have the genotype *er-105 erl1-2 erl2-1/+*; fisher's exact test, P<0.00000001.